REPORT DOCUMENTATION PAGE

1. AGENCY USE ONLY (Leave blank)	2. REPORT DATE July 14, 1995	3. REPORT TYPE AND DATES COVERED Technical Report 06/01/94 - 05/31/95

4. TITLE AND SUBTITLE
Chemical and Electrochemical Reactions in Porous Sol-Gel Materials

6. AUTHOR(S)
B.C. Dave, B. Dunn and J.I. Zink

5. FUNDING NUMBERS
Grant: N00014-93-1-0245
Dr. Robert J. Nowak
R&T Code: 4133041

7. PERFORMING ORGANIZATION NAME(S) AND ADDRESS(ES)
Department of Materials Science and Engineering
University of California, Los Angeles
Los Angeles, CA 90095-1595

8. PERFORMING ORGANIZATION REPORT NUMBER
Technical Report No. 4

9. SPONSORING/MONITORING AGENCY NAME(S) AND ADDRESS(ES)
Office of Naval Research
Chemistry Division
800 North Quincy Street
Arlington, VA 22217-5660

DTIC SELECTED
JUL 21 1995
G

10. SPONSORING/MONITORING AGENCY REPORT NUMBER

11. SUPPLEMENTARY NOTES
For publication in Fundamental Materials Research

12a. DISTRIBUTION/AVAILABILITY STATEMENT
This document has been approved for public release and sale; its distribution is unlimited.

12b. DISTRIBUTION CODE

13. ABSTRACT (Maximum 200 words)

Sol-gel synthesis approaches have enabled researchers to design composite-type materials where dopant molecules which carry out various types of chemical reactions are trapped in the nanopores of the host material. Dopant molecules have been shown to undergo chemical, photochemical and electrochemical reactions in the pores of sol-gel matrices with specific examples including complexation reactions, redox reactions, catalysis, protonation-deprotonation, isomerization and ion/electron transfer. The interconnected pore network of the xerogel or aged gel structure ensures that the molecules are responsive to the outside environment, yet the molecules are also trapped within the inorganic matrix which confines molecular motion and prevents their being leached from the matrix.

DTIC QUALITY INSPECTED 5

14. SUBJECT TERMS
Sol-gel synthesis, porous materials, reaction chemistry

15. NUMBER OF PAGES
19

16. PRICE CODE

17. SECURITY CLASSIFICATION OF REPORT Unclassified	18. SECURITY CLASSIFICATION OF THIS PAGE Unclassified	19. SECURITY CLASSIFICATION OF ABSTRACT Unclassified	20. LIMITATION OF ABSTRACT

OFFICE OF NAVAL RESEARCH

GRANT: N00014-93-1-0245

R&T Code: 4133041

Dr. Robert J. Nowak

Technical Report #4

Chemical and Electrochemical Reactions in Porous Sol-Gel Materials

by

Bakul C. Dave, Bruce Dunn and Jeffrey I. Zink

Department of Materials Science and Engineering
University of California, Los Angeles
Los Angeles, CA 90095-1595

Accesion For		
NTIS CRA&I		☒
DTIC TAB		☐
Unannounced		☐
Justification		
By		
Distribution /		
Availability Codes		
Dist	Avail and / or Special	
A-1		

July 14, 1995

19950720 037

CHEMICAL AND ELECTROCHEMICAL REACTIONS IN POROUS SOL-GEL MATERIALS

Bakul C. Dave,[1,2] Bruce Dunn,[1] and Jeffrey I. Zink[2]

[1]Department of Materials Science and Engineering
[2]Department of Chemistry and Biochemistry
University of California, Los Angeles
Los Angeles, CA 90095

INTRODUCTION

Solution phase reaction chemistry is largely a homogeneous discipline while the reactions carried out in the micropores of zeolites (pore size ~ 10 Å) and related compounds involve molecules placed in an ordered microheterogeneous environment. The outstanding properties of zeolites in the fields of size-specific absorption, molecular sieving and shape-selective catalysis have made these materials the focus of intense research activity over the last two decades.[1] The major drawback of their applications, however, has been the limitation of their pore size which excludes incorporation of a large number of molecular entities in these matrices. The most obvious approach to extend the chemistry and make it accessible to large molecules involves the use of porous host materials containing bigger pores.

One group of well-known and well-characterized porous materials is the SiO_2 gel structures obtained by the sol-gel route.[2] Two major reaction chemistry areas involving doped sol-gel materials have emerged over the past decade. First, the low-temperature solution-based sol-gel synthesis route has been found to be suitable for encapsulation of various organic, organometallic, and coordination compounds.[3] Second, the innovative use of buffered sol-gel procedures has made the encapsulation of biomolecules feasible in the nanopores of the silica gel glasses.[4] The added dopant molecules reside in the porous network of these sol-gel composite materials as a part of an organized supramolecular architecture.

This review is concerned primarily with the aspects of reaction chemistry in such sol-gel derived host media. The heterogeneous, multiphase reaction chemistry that is designed to occur in the porous structure of the host matrix constitutes the focus of this article. The unique state of aggregation of such sol-gel composites, where dopant molecules are dispersed in the

nanopores of the material, exemplifies a state intermediate between isotropic solution phase and the microporous zeolite media. Such a nanoporous system utilizes the properties of spatially arranged molecules in a solvent-rich environment and different molecules can be made to carry out various processes such as catalysis, charge transfer, electron transfer, and ion transport to generate specific chemical and electrochemical responses. This paper aims to describe and review a variety of reactions involving the organic, coordination, organometallic, and biological molecules encapsulated in sol-gel derived silica and vanadia gels. Specifically, the reaction chemistry of various dopant molecules in these matrices will be discussed.

OVERVIEW OF SOL-GEL CHEMISTRY

The sol-gel technique enables one to prepare a wide variety of oxide materials. In this approach, metal-alkoxides, (formula $M(OR)_n$, where M is Al, Si, Ti, V, Cr, Mo, W, etc. and R is an organic group) undergo hydrolysis followed by polycondensation reactions in solution at room temperature. The synthesis of oxides by this approach has been the subject of several reviews.[2,5-6] To date, silica-based systems have received the most attention.

The sol-gel process can generally be divided into the following stages: forming a sol, gelation, aging, drying and densification. The key feature in this sequence is sol-gel polymerization which can be described as a two-step reaction.[7] Initiation is performed via the hydrolysis of alkoxy ligands. This leads to the formation of hydroxylated M-OH groups:

$$M(OR)_n + H_2O \rightarrow \left[M(OR)_{n-1} OH \right] + ROH$$
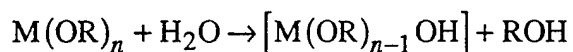
Propagation then occurs by the polycondensation of these hydroxylated species giving rise to oxypolymers. Polycondensation involves an oxylation reaction which, in turn, leads to the formation of oxo bridges and the removal of XOH species:

$$M-OH + M-OX \rightarrow M-O-M + XOH \quad (X = H \text{ or } R)$$
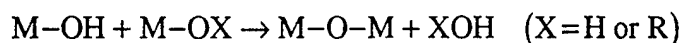
The chemical reactivity of metal alkoxides $M(OR)_n$ towards hydrolysis and condensation depends mainly on both the electrophilicity of the metal atom and its ability to undergo an increase in coordination number.[7] Silicon alkoxide $Si(OR)_4$ precursors have a low electrophilicity and their coordination number is stable. Thus, the hydrolysis of $Si(OR)_4$ is slow and their polymerization reactions are mainly controlled by the use of acid or base catalysis.

In sol-gel silica systems there is good understanding of the chemistry involved and how the reactions influence microstructural development.[1,5-6] In general, the processes of hydrolysis and condensation are difficult to separate. The hydrolysis of the alkoxide need not be completed before condensation starts and, in partially condensed silica, hydrolysis can still occur at unhydrolyzed sites. Several parameters are known to influence hydrolysis and condensation reactions including the temperature, solution pH, the particular alkoxide precursor, the solvent and the relative concentrations of each constituent.

The chemical conditions for hydrolysis and condensation of silicates have a prominent effect on gel morphology.[2,8] It is well appreciated that one can produce linear polymers, branched clusters or colloids in the solution depending upon various factors including the H$_2$O:Si ratio and pH. Silicate gels prepared at low pH (< 3) and low water content (< 4 mol water per mol of alkoxide) produce primarily linear polymers with low crosslink density. Additional crosslinks form during gelation and the polymer chains become increasingly entangled. Silicate gels prepared under more basic conditions (pH 5-7) and/or high water contents produce more highly branched clusters which behave as discrete species. Gelation then occurs by linking clusters together.

As hydrolysis and condensation reactions continue, viscosity increases until the solution ceases to flow. The time to gelation is an important characteristic which is sensitive to the chemistry of the solution and the nature of the polymeric species. The sol-to-gel transition is irreversible and there is little or no change in volume. At this stage, the one-phase liquid is transformed into a two-phase system. The gel consists of aggregates of colloidal particles (5 - 10 nm or smaller) with an interstitial liquid phase. After gelation, the gels are generally subjected to an aging process for a period of time lasting from hours to days. The gels are kept in sealed containers and very little solvent loss or shrinkage occurs. During the aging of silica gels, the condensation reactions continue, increasing the degree of crosslinking in the network, producing materials with increased mechanical strength and rigidity.

The experiments described in this paper were carried out either with aged gels or with xerogels. The latter are gels which have been dried, i.e., the interstitial pore liquid is removed, usually by low temperature evaporation, after the aging treatment. There is considerable weight loss, the gel shrinks substantially and the pore size decreases accordingly. As evaporation occurs, drying stresses arise which can cause catastrophic fracture of these materials.[9]

The sol-gel chemistry of transition metal alkoxides is more complicated.[7] Metal atoms not only have a high electrophilicity they can also exhibit several coordination states. Most alkoxides are highly reactive and precipitation occurs as soon as water is added. Thus, the synthesis of polymeric transition metal oxide based sols and gels requires careful control of the chemistry. Water used in the hydrolysis of alkoxides can be diluted in solvent or provided *in-situ* via a chemical reaction. Another approach is to design molecular precursors via chemical modification prior to their hydrolysis.[10] Since transition metal alkoxides react with nucleophilic reagents, they can be modified by using complexing ligands HOX (OX = acetylacetone, acetate):[11]

$$M(OR)_n + mXOH \rightarrow \left[M(OR)_{n-m}(OX)_m \right] + mROH$$
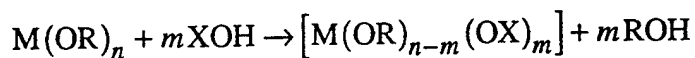
In this case the alkoxy groups (OR) are replaced by new ligands (OX) that are less easily removed upon hydrolysis. Thus, the alkoxy ligands are rather quickly removed upon hydrolysis while chelating ligands act as termination agents that limit condensation reactions.[12] By controlling the rates of hydrolysis and condensation through chemical modification, it is possible to prepare a given transition metal oxide in different forms such as colloids, gelatinous precipitates, colloidal gels and polymeric gels.[7] The gelation, aging and drying stages for sol-gel transition metal oxides are comparable to those described previously.

REACTIONS IN THE PORES OF THE SOL-GELS

A large number of dopant molecules has been shown to undergo chemical, photochemical, and electrochemical reactions in sol-gel glasses. These reactions include ligand exchanges, isomerization reactions, redox reactions, protonation-deprotonation, complexation, ion/electron transfer, and catalysis. Presently, there are a number of studies that have been reported in the literature (Table 1). Nevertheless, the basic mechanisms by which the porous structure influences these reactions remain largely obscure. One difficulty is the identification, description and control of experimental parameters such as pore size distribution, surface area and porosity, and the exact physical stage of the sol-gel material. Another difficulty is finding appropriate kinetic models for the porous reaction media. In spite of all these complications, some very fine investigations have been performed. Several recent studies have made very effective use of optical absorption and fluorescence spectroscopies and it is hoped that other techniques will soon be applied towards studying the reactions in these materials.

Table 1. Chemistry in Pores of Sol-Gel Materials

Features	Refs.
Acid-base	13
Proton Transfer	14
Photoinduced Charge Separation	15
Metal-Ligand Complexation	13a-c
Photo/Thermal Isomerization	16
Chemiluminescence	17b
Heterogeneous Catalysis	18
Surface Enhanced Raman Spectroscopy	19
Mediated Electron Transport	20
Electron-Ion Transport	21
Rigidochromism	22
Biocatalysis	4
Metalloenzyme-Ligand Binding	4a
Electrocatalysis	23
Affinity Interactions	24
Symmetry Lowering	25
Reversed-Phase Chemistry	26

Reactions occurring between different components inside the porous structure of the gel have received considerable attention in sol-gel chemistry. In this paper we review recent advances in sol-gel reaction chemistry with specific emphasis on chemical and electrochemical reactions of different sol-gel encapsulated species.

CHEMICAL REACTIONS

Acid-Base. The presence of an aqueous environment within the pores of the gels makes it highly feasible to carry out proton-transfer and acid-base reactions. One common theme in this field has been the study of pH indicator dyes.[13] Almost all the pH indicators that work in solution media have shown an unperturbed acid-base reaction chemistry in the porous gel media. One of the early studies involved the acid-base reactions of pH indicator dyes in the monolithic gels. Lev et al studied the proton dependent behavior of a series of indicator molecules including methyl orange, methyl red, bromocresol purple, phenol red, cresol red, phenolphthalein, and thymol-phthalein.[13b] The reactions of the various dyes encapsulated in sol-gels in the pH range of 0-11 were monitored using optical spectroscopy (Table 2).

Table 2. Colorimetric Response of Sol-Gel Encapsulated Acid-Base Indicators[a]
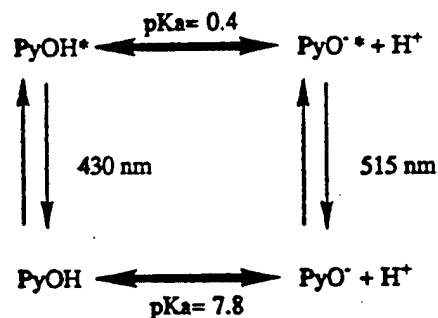
pH Indicator Dyes	Color Change	pH Range
Methyl Orange	Red→Yellow	0-2
Methyl Red	Red→Yellow	2.5-4.6
Bromocrsol Purple	Yellow→Purple	5.2-6.8
Bromothymol Blue	Yellow→Blue	6.2-7.6
Phenol Red	Yellow →Red	6.4-8.0
Cresol Red	Yellow→Red	7.2-8.8
Phenolphthalein	Colorless→Pink	8-10
Thymolphthalein	Cololess→Brown	9.4-10.6
Nile Blue	Blue→Red	9.5-10.6

[a]adapted from refs. 13a and 13e.

A detailed study of pH dependent reactions for different fluorescein dyes in sol-gel thin-films has been reported.[13d] The pH dependent optical response of cationic, neutral, anionic, and dianionic forms of the sol-gel encapsulated dye was monitored. The optical responses of the different forms of the dye were found to be similar to those in solution. Due to a direct correlation that exists between the optical response and pH of the medium, the sol-gel glasses doped with indicator dyes are mainly used as pH sensor elements. The main attraction of these materials is the prospect of an improvement in stability over the pH electrode. However, due to limited pH sensitivity away from the pK_a of the indicator, the range available for detection is restricted. Nonetheless, for a specific application within a known pH range these sensors appear quite promising.

Proton-Transfer. In spite of a large body of work existing in the area of sol-gel encapsulation of acid-base dyes, reaction kinetics of proton-transfer reactions in sol-gel media are not well characterized. In general, the absorption properties of the acid-base dyes are due to an extensive electron delocalization and its control by the proton-transfer reactions. The effects of encapsulation in a matrix capable of supporting acid-base (pK_a of silica ~1.7), and H-bonding

interactions are not well understood at present. Our focus in this direction has been to assess the influence of the matrix on the acid-base chemistry and the kinetics of proton transfer reactions. Described below are the reaction kinetics of excited state proton recombination reactions of pyranine (8-hydroxy-1,3,6-trisulfonated pyrene).[14]

$$\text{PyOH}^* \underset{\text{pKa= 0.4}}{\longleftrightarrow} \text{PyO}^{-*} + \text{H}^+$$

$$\big\updownarrow 430 \text{ nm} \qquad \big\updownarrow 515 \text{ nm}$$

$$\text{PyOH} \underset{\text{pKa= 7.8}}{\longleftrightarrow} \text{PyO}^- + \text{H}^+$$

The differences in the pK_a between the ground ($pK_a = 7.8$) and excited state ($pK_a = 0.4$) of the pyrene molecule provide a basis to study the kinetics of the proton transfer reaction between the ground and the photoexcited states. Upon photoexcitation, the molecule is deprotonated and when the molecule relaxes back to the ground state it recombines with the proton to generate the original form. In this way, a two-laser pump-probe technique can be used to monitor the dynamics of the reaction. The pump laser (excimer laser, $\lambda = 308$ nm) was used to generate the photoexcited deprotonated form of the dye. The proton recombination reaction was monitored with a cw Kr^+ laser ($\lambda = 476$ nm) which followed the changes in absorbances as a function of time. The absorption response essentially measures the optical density changes due to the back-protonation reaction in the time domain. Thus, the results of absorption decay experiments can be used for kinetic analysis and measurement of the rate constant of the protonation reaction.

$$\ln\left[\, x_o\big(x_t + [H^+]_o\big)\right] \Big/ \left(x_t\big(x_o + [H^+]_o\big)\right)\right] = k\left[H^+\right]_o t$$

The second-order rate constants obtained from the kinetic analysis reveal relatively little change in the proton-transfer kinetics existing in aqueous solution ($k = 8.5 \times 10^{10} \, M^{-1} \, s^{-1}$), sol ($k = 7.9 \times 10^{10} \, M^{-1} \, s^{-1}$), and aged gel ($k = 7.6 \times 10^{10} \, M^{-1} \, s^{-1}$). The rate constant for the xerogel, however, is reduced slightly ($k = 4.6 \times 10^{10} \, M^{-1} \, s^{-1}$). The activation energy for the back-protonation reaction was estimated by using a plot of the natural log of the rate constant versus reciprocal temperature. The activation energy for the reaction in the sol-gel medium was found to be 2.4 times higher (8.4 kcal/mol) as compared to the value observed in aqueous solution (3.5 kcal/mol). The observed activation energy is still more reflective of a solution phase as compared to values observed in the solid state. The increase in activation energy was attributed to diffusion related processes. It was concluded that proton diffusion inside the gel takes place via a pathway involving H-bond migration such that proton transfer occurs along the interior surface of the pores.[14] The rate constant data provide the most direct evidence so far about the reaction dynamics of the proton-transfer reaction in sol-gel media. The rate evidence strongly suggests an ability for the sol-gel porous materials to carry out acid-base reactions effectively, at least as far as low molecular weight organic dyes are concerned.

Electronn Donor-Electron Acceptor. Analogous to the acid-base and proton-transfer reactions, donor-acceptor reactions should also be feasible within the sol-gel matrices. The photoinduced electron-transfer reactions between sol-gel immobilized donor and acceptor molecules have been reported by Slama-Schwok et al.[15] The photoinduced electron transfer reactions studied involve a mobile mediator molecule, which acts as a mediator of charge between the immobilized donor and acceptor molecules. The authors initially studied the photoinduced electron transfer reaction between immobilized Ir(III) and Ru(II) complexes.[15a] The organic molecule 1,4-dimethoxybenzene (DMB) was used as a mediator molecule. The electron transfer from the donor to the acceptor molecule was carried out in two steps; the first one involving electron transfer from DMB to the photoexcited Ir(III) complex, and the second one from Ru(II) to the DMB$^+$ ion. The same group also reported a similar system based on immobilized pyrene as electron donor, methyl viologen as electron acceptor, and the N,N'-tetramethylene-2,2'-bipyridinium ion as the mobile electron shuttler.[15b] This system is reported to exhibit a long-lived charge separation suggesting an inhibited back-electron transfer reaction. According to the authors, the long-life of the charge separated state is a consequence of the matrix that immobilizes the donor and acceptor molecules, and physically separates them in the pores of the sol-gel materials. The use of constrained media to influence the rate of back-electron transfer reactions has been covered extensively in the literature, and the results of Slama-Schwok et al[15b] are in general agreement with the influence of medium on the rates of electron transfer.

Metal-Ligand Complexation. The porous architecture of the sol-gel glasses is such that it allows diffusion of low molecular weight species in and out of the gels. If suitable ligands are trapped in the sol-gels, they can be made to react with metal ions from an external solution upon immersion in that solution. Based on this principle, Zusman et al prepared a range of colored metal complexes inside sol-gel glasses.[13a] The ligands were immobilized in the gels and the gels were then allowed to dry. Upon immersion of these xerogels into solutions containing metal ions, characteristic colored complexes could be formed. The formation of these complexes was monitored by optical spectroscopy techniques.

Initial work in this area by Avnir and coworkers focused on adaptation of complexometric analytical reactions to sol-gel glasses.[13a-c] They were able to generate the red colored Fe(II) phenanthroline complex inside the xerogel network by either trapping the Fe^{2+} ion in the gel and diffusing the ligand, or alternatively, by immobilizing the ligand and then reacting it with an external solution containing the Fe^{2+} ion. In both cases the reaction was found to initiate rapidly (within 2 s). The reaction was found to proceed with high sensitivity for Fe^{2+} and the authors were able to spectrophotometrically detect sub-ppb levels of divalent iron.

$$Fe^{2+} + 3\,(o\text{-phen}) \rightarrow Fe(o\text{-phen})_3{}^{2+}$$
$$\text{clear} \qquad\qquad\qquad \text{red}$$
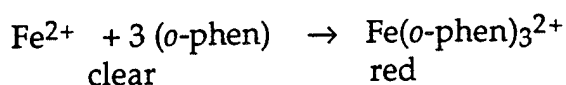
Similar chemistry with other metal ions such as Co^{2+}, Cu^{2+}, Ni^{2+}, and Pb^{2+} was also shown by the same group.[13a,b] Complexation reaction of the α-

benzoin oxime (Cupron) trapped in a xerogel with external solution containing Cu^{2+} ions at elevated pH (8-10) was found to proceed within 1 s. The formation of the green color could be correlated spectrophotometrically with the concentration of the Cu^{2+} ion. Similar chemistry was also demonstrated with complex formation reactions of Co(II) with α-nitroso-β-naphthol as the ligand, with Ni(II) dimethylglyoxime complex, and with reactions of Pb^{2+} with gallocianine. The reactions monitored by optical spectroscopy showed faster reaction time for Ni^{2+} (1 s) while the reaction times for the Co^{2+} and Pb^{2+} (15-30 min.) were found to be much slower.

Quantitative determination of complexation reaction kinetics in sol-gel doped systems is usually hampered by leaching out of the immobilized ligands from the gel upon immersion in an aqueous solution. However, Lev et al found that the o-phenanthroline ligand was immobilized very efficiently in the gels.[14] They found that only a negligible fraction (< 0.3 %) of the sol-gel encapsulated ligand was able to leach out even after 10 days of immersion in distilled water. This system was, therefore, pursued as a model system in which to carry out a detailed mathematical analysis of the complexation equilibria in gel glasses. The research approach involved obtaining model equations based on certain simplifying assumptions for the complexation kinetics in the gels and mathematically simulating the reaction profile of Fe^{2+} with the immobilized o-phenanthroline ligand.[13b]

The ease of optically monitoring the formation of colored complexes in the transparent gels enables these systems to be considered for solid state gel-based optical sensor elements. Due to the transparency of the gel matrix, analytical detection tests may be performed visually as well as spectrophotometrically. The reaction chemistry in the nanoporous gel is analogous to the solution phase reactions and these systems extend classical solution based analytical detection methodologies to a portable solid state matrix.

Isomerization. The ability of the finite sol-gel reaction cavity to influence the reaction dynamics of unimolecular reactions is nicely illustrated by the isomerization reactions of azobenzene dyes. Ueda et al studied the photoinduced *trans-to-cis* isomerization and the thermal *cis-to-trans* conversion in sol-gel derived materials.[16] The results for this reaction provide important conclusions about the porous structure and the reactions occurring within the porous sol-gel material.

In the isomerization studies of azobenzene dyes by Ueda et al,[16] the reaction rates are not perturbed in aged gels whereas in xerogel films striking deviations from first-order kinetic behavior are observed. The *trans-to-cis* photoisomerization of *trans*-4-methoxy-4'-(2-hydroxyethoxy)azobenzene (*trans*-MHAB) encapsulated in aged sol-gels was found to be almost identical to the conversion rates observed in aqueous ethanolic solutions. Irradiation (365-nm light) of the solution as well as the gel samples containing the *trans* isomer with was found to accompany a photoconversion to the *cis* form with ~90% of the *cis* product in a photostationary state. The fraction of the *cis* form produced in aged sol-gels was found to be almost identical (within the limits of experimental errors) to that in solution.[16b]

The thermal isomerization of the *cis-to-trans* form in aged gels was also reported by these authors.[16b] The thermal isomerization of the MHAB obeys first order kinetics and reveals that virtually no changes in the reaction kinetics are observed even though the molecule is entrapped in solid bulk material.

This reflects ample availability of free volume in the nanoporous reaction cavity of the aged gel such that the isomerization of the azo dye takes place as readily as in solution. These experiments suggest that the silica gel nanoporous structure is able to support at least unimolecular reactions of organic molecules in its pores with reaction kinetics comparable to the solution phase.

The same authors also reported on the photoisomerization of *trans*-MHAB in sol-gel derived silica films.[16a] While the aged monolithic gels contain larger pores, xerogel films show a pore distribution favoring small pore diameters and important differences in the reaction rates are observed. Irradiation of solution-based samples and sol-gel films incorporating the *trans* isomer of the dye was carried out with 365-nm light. Under steady-state conditions, the solution based samples showed 92-93% *cis* isomer fraction while the sol-gel samples showed a considerably reduced fraction of the *cis* isomer (~60%). The photoconversion to the *cis* form in the sol-gel films was found to be a function of the sample preparation conditions which are likely to determine the resulting pore sizes and distribution. The suppression of photoisomerization shows the influence of the porous reaction cavity in affecting the reaction kinetics of the dopant molecules. The thermal isomerization reaction of the *cis*-to-*trans* form of the *cis*-MHAB dye was also found to deviate significantly from the first order kinetics observed in solution.[16b]

These studies clearly illustrate the influence of the porous structure of the gel and the reaction cavity in which the reactant resides. Drying of the gels leads to shrinkage of the pores and the pore diameters attain nanometer dimensions (~40-50 Å). Xerogel films contain even smaller pore diameters, and the matrix begins to assert an influence on shape-selective phenomena. The *trans*-to-*cis* isomerization reaction of the azo dye requires that sufficient free volume be available in the reaction cavity. The changes in the reaction rates for the photoisomerization process in the xerogel medium are ascribed to confinement effects of the porous medium, with the matrix raising the activation energy needed for the reaction to proceed. The gel medium, therefore, promotes chemistry analogous to solution in the aged gel form while in the xerogel state the gel matrix begins to influence the reaction chemistry.

Chemiluminescence. Light emitting chemical reactions have a wide range of applications.[17a] In chemiluminescence reactions, chemical energy generated as a result of the decomposition of a weak bond produces excited-state intermediates that decay to a ground state with the emission of light. Luminescence properties of molecules are strongly medium dependent and it is of interest to observe whether such properties can be preserved in the sol-gel environment. The chemiluminescent molecule that was studied in sol-gels is luminol (5-amino-2,3-dihydro-1,4-phthalazinedione).[17b] Upon reaction with a $NaOH-H_2O_2$ solution chemiluminescence can be initiated. The luminol molecules were trapped in the sol-gel glasses and their reaction with the basic peroxide solution was monitored.

The luminol molecules were found to retain their chemiluminescent properties in the sol-gel host. In general, the light emitting properties of luminol were retained in the gel although the intensity of the emission was reduced in the xerogels by a factor of six. The initiation and subsequent decay of the chemiluminescence reaction were monitored in the solution (DMSO) as well as in silica xerogels. From this, the time constants for decay of the

emission intensity were calculated. It was found that, for the xerogels, the luminescence decay was slightly slower in the xerogels (283 s) as compared to DMSO (206 s) solution. The prolonged lifetime of the luminol molecules suggests a relative stabilization of the light emitting excited state by the xerogel environment.[17b]

The luminescence properties are strongly medium dependent and the emission maxima provide a convenient assessment of the reaction microenvironment for the chemiluminescent molecule. In purely aqueous media, luminescence occurs at 424 nm, while in DMSO it shows a maximum centered at 485 nm. The chemiluminescence in the sol-gel encapsulated luminol occurs closer to the region observed for aqueous media and suggests a predominantly water-rich reaction medium available to the molecule in the sol-gels. The sol-gel matrix thus serves as an efficient host for chemiluminescent reactions.[17b] Light emitting reactions form the basis for a wide range of chemical and biochemical detection assay systems and the feasibility of these reactions in a solid state medium may provide the necessary impetus for supporting its development as a core analytical technique.

Chemical Catalysis. The application of sol-gel related catalysis techniques has been largely based upon use of sol-gel immobilization of catalytically active species.[18a] Preliminary efforts carried in this direction were by Gomez and coworkers who synthesized a series of catalyst materials involving Ru, Pt, and Pd dispersed in silica.[18b] These metal catalysts were added directly to the sol-gel reaction mixture for encapsulation purposes.

In their study Gomez and coworkers used square planar complexes of the type trans-$[M(NH_3)_2Cl_2]$ where M = Pt or Pd to incorporate these metals in the sol-gel structure.[18b] FTIR and UV-vis spectroscopies were used to characterize the nature of the species incorporated in the gels. It was found that under conditions of acidic catalysis the tetrachloro anion of the metal was formed while under basic conditions tetraamino complex was isolated. Thus, the forms of the metal complexes that were trapped in the porous structure depended on the synthesis condition. Ru metal insertion in the silica gel was also accomplished by the Lopez et al using $RuCl_3$ as precursor dopant during the sol-gel polymerization reaction.[18c] Based on the FTIR data the authors concluded that part of the metal can be inserted into the silica network as Si-O-M. As hydrogenation catalysts, these encapsulated metallic particles were found to be superior to silica adsorbed catalysts because of their low rates of deactivations.

An analogous procedure was also adopted by Tour et al to generate sol-gel materials containing encapsulated Pd(0) particles.[18d] Their approach involved use of Pd(II) acetate in the sol-gel mixture. After gelation the solvent was removed under vacuum and a glassy black xerogel containing Pd(0) could be isolated. Such a catalyst was found to be selective towards hydrogenation of alkynes to alkenes. Selective hydrogenation of terminal double bonds that preserved the integrity of inner double bonds could also be achieved. Oxide catalyst particles trapped within the sol-gel porous structures were obtained by Ueno and coworkers.[18e,f] Their strategy involved addition of $Fe(NO_3)_3$ to the gelation reaction mixture and heating the resulting light yellow-brown gels to obtain oxide particles. By this approach metallic particle dispersions could also be obtained if the gel were heated under hydrogen atmosphere at 450 °C. The iron catalyst can be used for ammonia synthesis, Fisher-Tropsch synthesis and

for water gas shift reaction. Such catalysts are useful because of their easy recyclability. Finally, Avnir and coworkers have also recently reported direct sol-gel encapsulation of quaternary ammonium salts of Ru, Rh, Ir, and Pt which act as heterogeneous catalysts for bond isomerization, hydrogenation, hydroformylation, and disproportionation reactions in the sol-gel matrix.[18g]

Surface Adsorption. One of the new directions in sol-gel chemistry has been its novel application in the area of metal particle entrapment and surface related chemistry. The pores of the silica gel matrix serve as an appropriate host for formation of metal particle centers. As mentioned previously most of the research on metal particle encapsulation has focused on generation of metal nuclei from precursor molecules mixed in with the sol-gel reaction mixture. The metal particles can be generated chemically, or alternatively, via photolysis of precursor molecules as employed by Akbarian et al.[19]

An interesting application of metal particle entrapment was the use of photogenerated gold particles for surface adsorption of organic molecules for surface enhanced Raman spectroscopy (SERS). For this purpose, the precursor molecules of choice employed were dimethyl(trifluoroacetylacetonato)gold, $(CH_3)_2Au(tfac)$, and dimethyl(hexafluoroacetylacetonato)gold, $(CH_3)_2Au(hfac)$. Typical preparation of gold particles involved mixing the precursors with the sol-gel reaction mixture to generate gels containing the precursor molecules. The gold particles can then be directly generated within the pores of the gels by irradiation of these gels with 351-nm laser light or light from an unfiltered 100 W mercury vapor lamp. The size of the particles is governed by the intensity and duration of the irradiation and can be monitored by absorption spectroscopy. Thus, by careful control of irradiation, the desired particle sizes could be obtained. The characteristics of these gold particles were investigated by X-ray diffraction, and transmission electron microscopy which revealed the presence of gold particles of varying morphologies. The morphological features were found to be a function of the irradiation treatments.
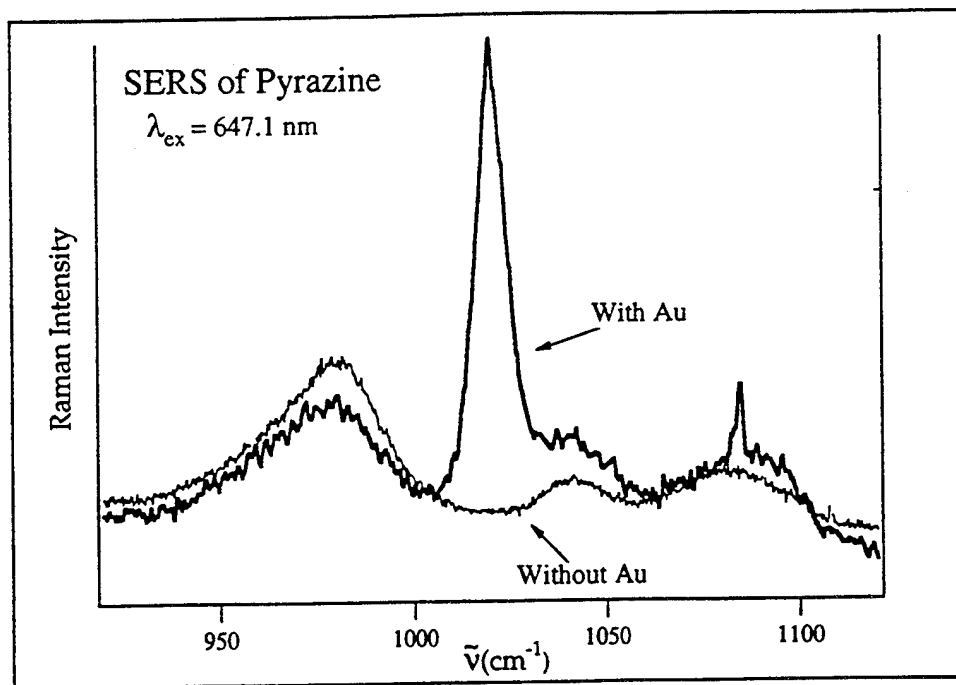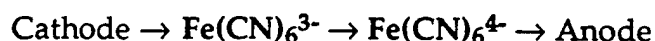

Figure 1. Raman spectra of sol-gel encapsulated pyrazine showing the SERS enhacement.

The gold particles generated in the pores of the sol-gel matrix were used to induce SERS activity in pyrazine molecules. For this purpose, the totally symmetric ring breathing mode of the pyrazine molecule at 1020 cm^{-1} was monitored with and without the presence of gold particles. Upon excitation of these samples with the 647.1-nm laser line, an increasingly intense vibrational mode at 1020 cm^{-1} was observed when the spectra were taken in gels containing the encapsulated gold particles (Fig. 1). The enhancement effect can only be attributed to surface adsorption of the pyrazine molecules on the gold particles, and in turn, provides evidence for the surface adsorption and charge transfer interactions operative in the gel matrix. The observed enhancement effects are also important from the point of view of enhanced vibrational spectroscopic sensitivity and selectivity. The SERS approach provides an improved means for detection of low concentration species, and holds promise for using sol-gel materials as optically-based vibrational sensors.

ELECTROCHEMICAL REACTIONS

Mediated Electron Transport. The isolation of a liquid phase in the pores of the solid gel matrix makes this constituent available for solution chemistry approaches which can be utilized for fast electron transport. As such, the wet gels represent an intriguing class of biphasic materials for carrying out aqueous redox-based reaction chemistry. Due to the interconnected porous structure of the gel matrix, the redox-active molecular species are generally mobile. As opposed to ionic charge transport, redox-mediated electron transport does not accompany extensive mass transfer. The gels doped with redox-active molecules can be considered as solid electrolytes designed to have an electronic current flowing in an external circuit through connected metal electrodes. The external current is balanced by an ionic-electronic current in the internal circuit. In its simplest configuration, the experiment constitutes monitoring the electrical response of a gel sample separated by two gold metal electrodes at the two ends of the monolith.

One objective with this research direction has been to use mobile redox-active ions as carriers of charge and electrons across the material.[20] The solution phase available in the porous gel structure ensures sufficient flexibility to incorporate a variety of redox-active molecular ions. The electron transfer to and from the electrodes was mediated by Fe(CN)$_6$$^{4-/3-}$ couple incorporated into the gel. The two-electrode two-terminal electrical response of the sol-gel sample containing ferrocyanide ions is shown in Fig. 2. The quasi-linear response in the low-overpotential domain (-0.4 to 0.4 V) suggests essentially ohmic behavior in this region. The overall electron flow for the reaction in this case can be written as

$$\text{Cathode} \rightarrow \text{Fe(CN)}_6{}^{3-} \rightarrow \text{Fe(CN)}_6{}^{4-} \rightarrow \text{Anode}$$

where electron transport within the gel matrix is mediated by the Fe(CN)$_6$$^{4-/3-}$ couple. The equilibrium and the fast self-exchange reactions of the redox-couple ensure minimal concentration polarization mass transport. The redox-molecules are believed to transport electrons within the gel through a series of intermolecular outer-sphere electron transfer events. In other words, electron transport through the bulk of the material occurs by local migration and subsequent self-exchange between the two forms of the redox active anion. The

electron transfer from one electrode to the other is thus very much similar to the valence-hopping mechanism observed in mixed-valence conductors.
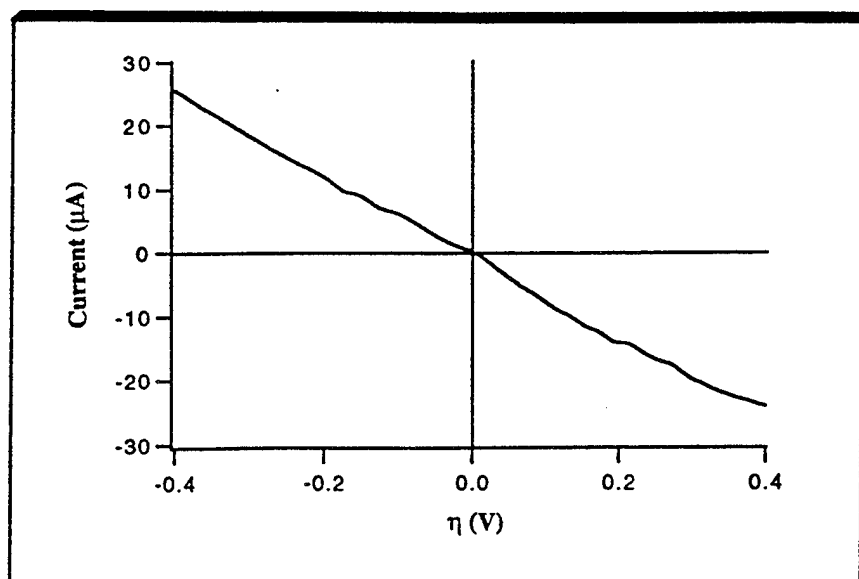

Figure 2. Ohmic response in low-overpotential region showing mediated electron transport in silica sol-gel.

Another very interesting feature observed in this system is that the anodic current response in this case is directly proportional to the concentration of the ferrocyanide present in the medium. If this reaction is coupled with another redox reaction, then changes can be produced in the equilibrium of the $Fe(CN)_6^{4-/3-}$ couple. Coupling this reaction with another redox reaction can be expected to cause changes in the overall concentration of the ferrocyanide ion in the medium. If the catalytic reactions of the enzymes are coupled with this reaction then the rate and extent of catalysis can be monitored by the electrical response of the system.[20]

In order to test the influence of catalytic reactions on the electrochemical properties of the sol-gel immobilized $Fe(CN)_6^{4-/3-}$ mediators the electrical response of the system was obtained in the presence of enzymes under catalytic conditions. The equilibrium shift of the $Fe(CN)_6^{4-/3-}$ couple perturbed by the biocatalytic reaction leads to changes in the electrical properties of the sol-gel medium. Two different enzyme systems, namely, horseradish peroxidase (HRP) and alcohol dehydrogenase (ADH) were coupled to the ferri/ferrocyanide electron transport reaction.[20]

The heme containing enzyme, HRP, catalyses the reduction of peroxide to water using a suitable electron donor such as ferrocyanide.

$$2\,H^+ + 2\,Fe(CN)_6^{4-} + H_2O_2 \xrightarrow{\text{HRP}} 2\,H_2O + 2\,Fe(CN)_6^{3-}$$

In this reaction, as a result of enzymatic catalysis the concentration of the ferrocyanide is diminished in the system and less current is generated by the anodic reaction (Fig. 3). The loss of current suggests an effect of the catalytic reaction on the ferri/ferrocyanide equilibrium. The electrons being used up as a result of the catalytic reaction cause a decrease in the overall current flowing

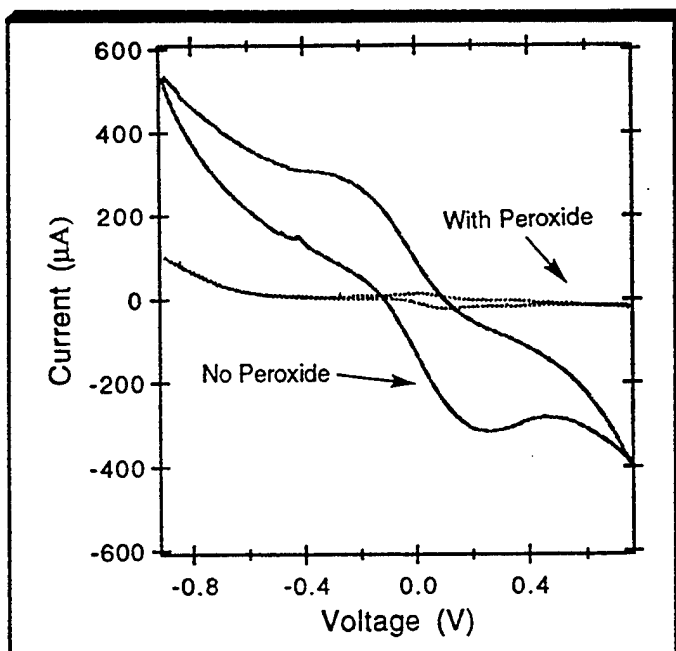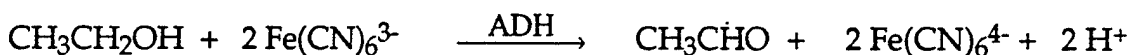through the cell, and a decrease in output currents is observed for a given applied overpotential.

Figure 3. Electrochemical response of peroxide biocatalysis by HRP in silica sol-gel.

Alternatively, coupling of the ADH catalytic reaction

$$CH_3CH_2OH + 2\,Fe(CN)_6^{3-} \xrightarrow{\ \ ADH\ \ } CH_3CHO + 2\,Fe(CN)_6^{4-} + 2\,H^+$$

with the mediator couple leads to an increased concentration of the ferricyanide entity in the sol-gel medium. Upon exposure of the gels containing immobilized ADH and mobile $Fe(CN)_6^{4-/3-}$ molecules to ethanol vapor, the electrical response of the gel shows an effective increase as compared to that observed in the absence of ethanol.[20]
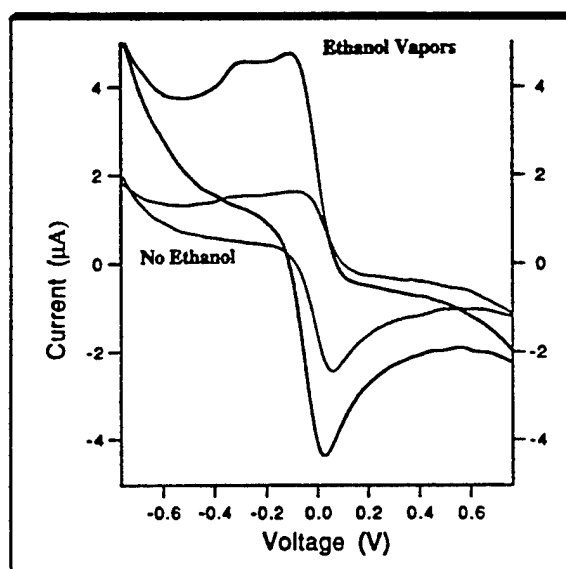

Figure 4. Electrochemical response of ethanol biocatalysis by ADH in silica sol-gel.

The oxidation of the ethanol vapors caused by the ADH enzyme results in liberation of excess electrons in the medium which is manifest as an increase in current for a given overvoltage. These results prove that coupled biocatalytic reactions are feasible in the sol-gel media. An especially attractive feature of this chemistry is that the electrons generated at the immobilized enzyme site are carried on to the distant electrodes by the mobile mediators. These experiments also prove the validity of biocatalytic reactions in the sol-gel media and the ability of the mobile mediators to effectively shuttle electrons between the redox site of an immobilized enzyme and the electrodes. In view of the dependency of the electrical response upon the concentration of the external molecules (peroxide, ethanol), it is likely that these systems will find a wide range of applications as sol-gel based biosensors.[4b]

Electron-Ion Transport. The use of sol-gel synthesis methods for electrochemical materials has been reviewed previously.[21] One aspect of this work which relates to the theme of chemical reactions in porous structures is the sol-gel synthesis of ion insertion compounds. In this regard, vanadium pentoxide xerogels have emerged as extremely promising cathode materials for solid-state lithium secondary batteries. The interest in this material is based on the reversible intercalation of lithium ions between the layers of the two-dimensional xerogel structure.

Vanadium pentoxide gels are commonly synthesized by aqueous routes to produce materials with the general composition $V_2O_5 \cdot n\ H_2O$.[27] These gels are composed of ribbon-like particles some 10 nm wide and several hundred nm long. When prepared as films, the oxide layers stack parallel to each other giving rise to one-dimensional order along a direction perpendicular to the substrate. The basal distance, d, between oxide layers depends on the amount of water contained within these layers. This distance increases in steps of 2.8Å, consistent with the van der Waals diameter of a water molecule. For V_2O_5 xerogels dried in ambient, the composition is $V_2O_5 \cdot 1.8\ H_2O$ and $d = 11.6$Å. Heat treatment at 120°C produces a smaller d value ($d = 8.8$Å) and corresponds to $n = 0.5$. The basal distance swells to $d = 17.7$Å for $n = 6$ and three water layers.

This one-dimensional swelling characteristic enables vanadium pentoxide gels to intercalate a wide variety of inorganic and organic guest species.[21,27] The chemically bound water in the intralamellar space can ion exchange with molecular ions such as long-chain alkyl-ammonium or ferrocenium,[28] participate in acid/base reactions, and readily intercalate metal cations such as lithium.[29] The ability to intercalate organic monomers produces novel organic-inorganic hybrid materials containing monolayers of conductive polymers in the intralamellar space between the vanadium oxide layers.[30]

The investigations of vanadium oxide xerogels as secondary cathodes for lithium batteries is part of the recent interest in the reversible intercalation of lithium in two-dimensional transition metal oxide host lattices. $V_2O_5 \cdot n\ H_2O$ gels are mixed conductors. The ability of this material to support Li^+ conduction is evident from its intercalation behavior while electronic conduction through the oxide network arises from electron hopping between V^{4+}/V^{5+}. Electrochemical lithium insertion occurs with compensating electrons as follows:

$$V_2O_5 + xLi^+ + xe^- \leftrightarrow Li_xV_2O_5$$
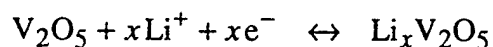
The high redox potential, wide range of lithium intercalation (value of x) and ease of fabrication have made V_2O_5 xerogels extremely attractive materials for thin film lithium batteries.[31] Whereas crystalline V_2O_5 has limited insertion (x < 1) and a discontinuous discharge curve, V_2O_5 xerogels exhibit substantially greater insertion (x = 1.5 to 2.0) and a continuous discharge curve with a large plateau between 3.5 V and 2.0 V.[29,31] A recent publication reported that more than 3 moles of lithium per mole of V_2O_5 could be inserted reversibly between 3.5 V and 1.6 V for 1000 cycles with no change in electrochemical behavior.[32] This significant increase in lithium capacity was attributed to both the microstructural characteristics of the films and their high surface area.

An important consideration for the vanadium oxide xerogels is the structural change occurring in the intralamellar space during intercalation. The aprotic electrolyte used in the electrochemical experiments, propylene carbonate, is believed to exchange with water molecules contained in the structure, swelling the basal spacing to d = 21.6 Å.[29] As lithium insertion occurs, (0.1 < x < 0.2) the organic solvent is expelled and the spacing decreases (d = 10.6Å). The chemical diffusion of lithium ($\tilde{D}_{Li}$) is strongly affected by this structural change. For low values of intercalation (x < 0.2), $\tilde{D}_{Li}$ is 10^{-8} - 10^{-9} cm^2/s, considerably greater than that observed for chemical diffusion in crystalline V_2O_5. When the structure collapses upon further intercalation, $\tilde{D}_{Li}$ decreases rapidly to the range of crystalline V_2O_5, ~ 5 x 10^{-11} cm^2/s (at x ~ 0.4) and then remains at this value with additional intercalation. It is interesting to note that the one-dimensional stacking of the vanadium oxide ribbons becomes increasingly disordered with greater intercalation levels.
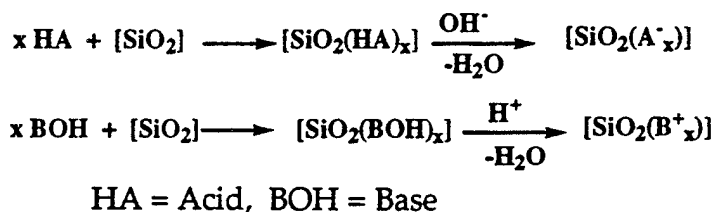
In related work, the sol-gel process has been used to prepare vanadium oxide aerogels.[33] These highly porous materials (> 80% porosity) are synthesized using a supercritical drying process. The ability to obtain extremely high surface areas (300 - 400 m^2/g) with this approach is of interest because higher surface areas are expected to lead to greater lithium insertion.[28] Since the solid phase of aerogels consists of small 3 - 5 nm particles linked in a three dimensional network, the electrochemistry which occurs in the solid phase is a nanodimensional process. Initial results indicate that these nanodimensional materials exhibit reversible intercalation of lithium.
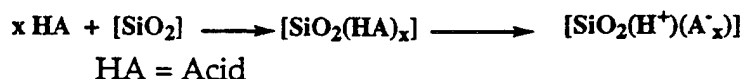
CONCLUSION

Sol-gel synthesis approaches have enabled researchers to design composite-type materials where dopant molecules which carry out various types of chemical reactions are trapped in the nanopores of the host material. Dopant molecules have been shown to undergo chemical, photochemical and electrochemical reactions in the pores of sol-gel matrices with specific examples including complexation reactions, redox reactions, catalysis, protonation-deprotonation, isomerization and ion/electron transfer. For the most part, it appears that the reaction kinetics in the sol-gel matrix are different from the same reactions occurring in solution, on surfaces or in zeolite structures. The interconnected pore network of the xerogel or aged gel structure ensures

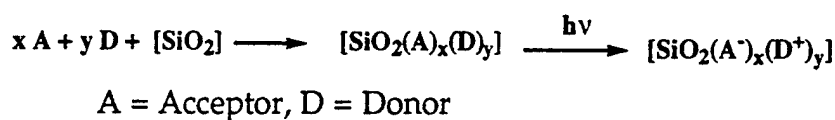**Table 1.** A Survey of Chemical Reactions Accesible within Sol-Gel Materials
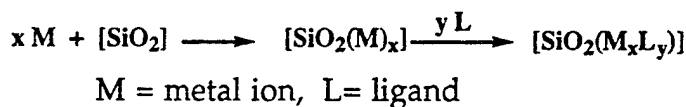
1) Acid-base

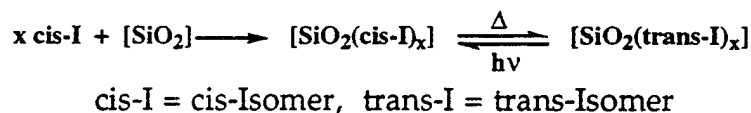$$x\,HA + [SiO_2] \longrightarrow [SiO_2(HA)_x] \xrightarrow[-H_2O]{OH^-} [SiO_2(A^-_x)]$$

$$x\,BOH + [SiO_2] \longrightarrow [SiO_2(BOH)_x] \xrightarrow[-H_2O]{H^+} [SiO_2(B^+_x)]$$

HA = Acid, BOH = Base

2) Proton Transfer

$$x\,HA + [SiO_2] \longrightarrow [SiO_2(HA)_x] \longrightarrow [SiO_2(H^+)(A^-_x)]$$

HA = Acid

3) Donor-Acceptor

$$x\,A + y\,D + [SiO_2] \longrightarrow [SiO_2(A)_x(D)_y] \xrightarrow{h\nu} [SiO_2(A^-)_x(D^+)_y]$$

A = Acceptor, D = Donor

4) Complexation

$$x\,M + [SiO_2] \longrightarrow [SiO_2(M)_x] \xrightarrow{y\,L} [SiO_2(M_xL_y)]$$

M = metal ion, L = ligand

5) Isomerization

$$x\,cis\text{-}I + [SiO_2] \longrightarrow [SiO_2(cis\text{-}I)_x] \underset{h\nu}{\overset{\Delta}{\rightleftharpoons}} [SiO_2(trans\text{-}I)_x]$$

cis-I = cis-Isomer, trans-I = trans-Isomer

6) Chemiluminescence

$$x\,Lum + [SiO_2] \longrightarrow [SiO_2(Lum)_x] \xrightarrow[H_2O_2]{NaOH} [SiO_2(Lum)_x] + h\nu$$

Lum = Luminescent molecule (Luminol)

7) Catalysis

$$x\,Cat + [SiO_2] \longrightarrow [SiO_2(Cat)_x] \longrightarrow [SiO_2(Cat)_x]$$

Substr   Prod

Cat = Catalyst

8) Surface Adsorption

$$x\,Au^0 + [SiO_2] \longrightarrow [SiO_2(Au^0)_x] \xrightarrow{C_aH_bN_c} [SiO_2(C_aH_bN_c)...(Au^0)_x]$$

$C_aH_bN_c$ = polarizable organic molecule

9) Redox /
   Electron Transport
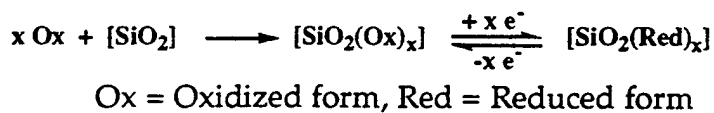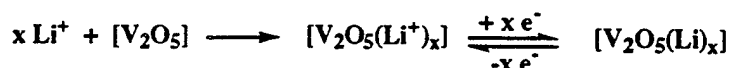
$$x\,Ox + [SiO_2] \longrightarrow [SiO_2(Ox)_x] \underset{-x\,e^-}{\overset{+x\,e^-}{\rightleftharpoons}} [SiO_2(Red)_x]$$

Ox = Oxidized form, Red = Reduced form

10) Electron-Ion Transport

$$x\,Li^+ + [V_2O_5] \longrightarrow [V_2O_5(Li^+)_x] \underset{-x\,e^-}{\overset{+x\,e^-}{\rightleftharpoons}} [V_2O_5(Li)_x]$$

that the molecules are responsive to the outside environment, yet the molecules are also trapped within the inorganic matrix which confines molecular motion and prevents their being leached from the matrix. This combination of factors offers the opportunity to study reactions under unique conditions and it is hoped that this review will promote further interest in the reaction chemistry which can be made to occur in these novel materials.

REFERENCES

1. H. van Bekkum, E. M. Flanigen, and J. C. Jansen, eds. *Introduction to Zeolites: Science and Practice* Elsevier, Amsterdam, (1991)
2. C.J. Brinker and G. Scherer, *Sol-Gel Science: The Physics and Chemistry of Sol-Gel Processing* Academic Press, San Diego, (1989).
3. (a) D. Avnir, D. Levy, and R. Reisfeld, *J. Phys. Chem.*, **88** (1984) 5956. (b) D. Avnir, S. Braun, and M. Ottolenghi, *Am. Chem. Symp. Ser.*, **499** (1992) 384.
4. (a) L. M. Ellerby, C. R. Nishida, F. Nishida, S. A. Yamanaka, B. Dunn, J. S. Valentine, and J. I. Zink, *Science*, **255** (1992) 1113. (b) B. C. Dave, B. Dunn, J. S. Valentine, and J. I. Zink, Anal. Chem., **66** (1994), 1120A. (c) D. Avnir, S. Brau, O. Lev, and M. Ottolenghi, *Chem. Mater.*, **6** (1994) 1605. (e) S. A. Yamanaka, F. Nishida, L. M. Ellerby, C. R. Nishida, B. Dunn, J. S. Valentine, and J. I. Zink, *Chem. Mater.*, **4** (1992) 495.
5. L. L. Hench and J. K. West, *Chem. Rev.*, **90** (1990) 33.
6. L. C. Klein, ed. *Sol-Gel Technology* Noyes Publications, Park Ridge, N.J. (1988).
7. J. Livage, M. Henry and C. Sanchez, *Prog. Solid State Chem.*, **18** (1988) 259
8. C. J. Brinker and G. W. Scherer, *J. Non-Cryst. Solids*, **70** (1985) 301
9. G. W. Scherer, *J. Non-Cryst. Solids*, **121** (1990) 104 and references therein
10. C. Sanchez, J. Livage, M. Henry and F. Babonneau, *J. Non-Cryst. Solids*, **100** (1988) 65.
11. B. E. Yoldas, *J. Mater. Sci.*, **21** (1986) 1087.
12. F. Ribot, P. Toledano and C. Sanchez, *Chem. Mater.*, **3** (1991) 759.
13. (a) R. Zusman, C. Rottman, M. Ottolenghi, and D. Avnir, *J. Non-Cryst. Solids*, **122** (1990), 107. (b) O. Lev, B. Kuyavskaya, Y. Sacharov, C. Rottmann, A. Kuselman, D. Avnir, and M. Ottolenghi, *SPIE. Proc. Ser.*, **1716** (1993) 357. (c) O. Lev, B. I. Kuyavskaya, I. Gigozin, M. Ottolenghi, and D. Avnir, *Fresnius J. Anal. Chem..*, **343** (1992) 370. (d) P. Lacan, P. LeGall, J. Rigola, C. Lurin, D. Wettling, C. Guizard, and L. Cot, *SPIE. Proc. Ser.*, **1758** (1992) 464. (e) M. Krihak, and M. R. Shahriari, *Chem. Mater.* In Press.
14. J. McKiernan, E. Simoni, B. Dunn, and J. I. Zink, *J. Phys. Chem.*, **98** (1994) 1006
15. (a) A. Slama-Schwok, D. Avnir, and M. Ottolenghi, *J. Am. Chem. Soc.*, **113** (1991) 3984. (b) A. Slama-Schwok, D. Avnir, and M. Ottolenghi, *Nature*, **355** (1992) 240.
16. (a) M. Ueda, H.-B. Kim, T. Ikeda, and K. Ichimura, *Chem. Mater.*, **4** (1992) 1229. (b) M. Ueda, H.-B. Kim, T. Ikeda, and K. Ichimura, *Chem. Mater.*, **6** (1994) 1771.

17. (a) L. J. Kricka, *Clin. Chem.*, **37-9** (1991) 1472. (b) F. Akbarian, B. S. Dunn, and J. I. Zink, *J. Mater. Chem.*, **3** (1993) 1041.

18. (a) M. A. Cauqui, and J. M. Rodriguez-Izquierdo, *J. Non-Cryst. Solids*, **147-8** (1992) 724. (b) T. Lopez, M. Moran, J. Navarrete, L. Herrera, and R. Gomez,*J. Non-Cryst. Solids*, **147-8** (1992) 753. (c) T. Lopez, L. Herrera, J. Mendez-Vivar, R. Gomez, and R. D. Gonzalez, *J. Non-Cryst. Solids*, **147-8** (1992) 753. (d) J. M. Tour, J. P. Cooper, and S. L. Pedalwar, *Chem. Mater.*, **2** (1990) 647. (e) S. Tanabe, T. Ida, M. Suginaga, A. Ueno, Y. Kotera, K. Tohji, and Y. Udagawa, *Chem. Lett.*, (1984) 1567. (f) T. Akiyama, E. Tanigawa, T. Ida, H.Tsuiki, and A. Ueno, *Chem. Lett.*, 91986) 723.

19. F. Akbarian, B. Dunn, and J. I. Zink, *J. Phys. Chem.* , **99** (1995). 3982.

20. E. H. Lan, B. C. Dave, B. Dunn, J. S. Valentine, and J. I. Zink, *MRS Symp Proc.* (1995).

21 (a) J. Livage, *Solid State Ionics* , **50** (1992) 307. (b) B. Dunn, G. C. Farrington and B. Katz, *Solid State Ionics*, **70-71** (1994) 3.

22. J. McKiernan, J.-C. Pouxviel, B. Dunn, and J. I. Zink, *J. Phys. Chem.*, **93** (1989) 2129.

23. (a) P. Audebert, C. Demaille, and C. Sanchez, *Chem. Mater.*, **5** (1993) 911. (b) P. Audebert, P. Griesmar, P. Hapiot, and C. Sanchez, *J. Mater. Chem.*, **2** (1992) 1293. (c) P. Audebert, P. Griesmar, and C. Sanchez, *J. Mater. Chem.*, **1** (1991) 699.

24. R. Wang, U. Narang, P. N. Prasad, and F. V. Bright, *Anal. Chem.*, **65** (1993) 2671.

25. D. Levy, R. Reisfeld, and D. Avnir, *Chem. Phys. Lett.*, **109** (1984) 593.

26. D. Levy, and D. Avnir, *J. Phys. Chem,*, **92** (1988) 4734.

27. J. Livage, *Chem. Mater.*, **3** (1991) 578.

28. P. Aldebert and V. Paul-Boncour, *Mater. Res. Bull.*, **18** (1983) 1263.

29. R. Baddour, J.P. Pereira-Ramos, R. Messina and J. Perichon, *J. Electroanal. Chem.*, **314** (1991) 81.

30. M. G. Kanatzidis, C. G. Wu, H. O. Marcy, D. C. DeGroot, and C. R. Kannewurf, *Chem. Mater.*, **2** (1990) 222.

31. K. West, B. Zachau-Christiansen, T. Jacobsen and S. Skaarup, *Electrochim. Acta*, **38** (1993) 1215.

32. S. Passerini, C. Chang, X. Chu, D. B. Le, and W. Smyrl, *Chem. Mater.*, **7** (1995) 780.

33. F. Chaput, B. Dunn, P. Fuqua and K. Salloux, J. Non-Cryst. Solids, in press.